17th World Conference on Earthquake Engineering, 17WCEE
Sendai, Japan - September 13th to 18th 2020

QUANTIFYING THE UNCERTAINTY IN MODELING OF RC WALLS

C. A. Arteta[1], J. Piedrahita[2], A. Ortiz[3], C.L. Segura Jr. [4], K. Kolozvari [5]

[1] *Assistant Professor, Universidad del Norte, Barranquilla (Colombia), carteta@uninorte.edu.co*
[2] *Graduate Student, Universidad del Norte, Barranquilla (Colombia), gjefferson@uninorte.edu.co*
[3] *Assistant Professor, Universidad del Valle, Cali (Colombia), albert.ortiz@correounivalle.edu.co*
[4] *Research Structural Engineer, National Institute of Standards and Technology, Gaithersburg, MD, USA, christopher.segura@nist.gov*
[5] *Assistant Professor, California State University, Fullerton, Fullerton, CA, USA, kkolozvari@fullerton.edu*

Abstract

Reinforced concrete (RC) walls are commonly used for buildings in regions of high seismicity to conform partly or totally their lateral load-resisting system. Among the features that influence the seismic response of RC walls are their geometry (e.g., I-, L- or C-shaped cross-section, cross-sectional aspect ratio), material properties, steel reinforcement detailing, confinement provisions, axial load ratio and shear span ratio. Several analytical models for nonlinear analysis of RC walls are available for research and design, programed based on different assumptions of material and/or element formulations (e.g. fiber- or strut-and-tie-based approaches, displacement- or force-based formulations with and without inelastic shear-flexure interaction). Studies have been conducted on the capability of these diverse approaches to simulate adequately the nonlinear behavior of RC walls with known experimental results, demonstrating their suitability for a wide range of engineering problems. However, other blind-prediction contests have also demonstrated that predicting accurately the actual response of a specimen under dynamic shaking is difficult, and the recorded dispersion in the results among team of experts is considerable; even when the geometric and material properties are well described, and the ground acceleration history is previously known. To determine the response sensitivity to variations in parameters of macroscopic models, sensitivity analysis based on Monte Carlo simulation is used through generation of plausible realizations in the Simcenter platform. RC wall specimen previously tested in the laboratory were used to validate two modeling approaches: (i) fiber forced-based model (FIBER), and (ii) the Nonlinear Truss model (NLT). For the NLT and the FIBER model, varied parameters for the formulations included material constitutive behavior of concrete and steel, axial load, mass, and damping ratio. The article quantifies the impact of modeling parameters in structural response, isolating in part, the record-to-record variability. Nevertheless, results indicate that the latter is the most important source of structural response variance.

Keywords: RC walls, seismic response, modeling uncertainty, EE-UQ, SimCenter.

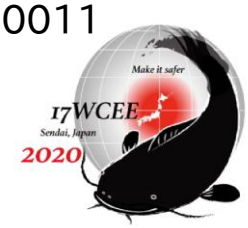

1. Introduction

Reinforced concrete (RC) walls are commonly used for buildings in high seismicity regions to partially or fully conform their lateral load-resisting system. The nonlinear nature of the RC walls response is now-a-days pushing the designers to use inelastic simulation to capture the broad range of plausible response when subjected to ground shaking of large intensity. Among the features that influence the seismic response of RC walls are their geometry (e.g., I-, L- or C-shaped cross-section, cross-sectional aspect ratio), material properties, steel reinforcement detailing, including confinement properties at the boundaries, axial load ratio (ALR = $P/A_g f'_c$), and shear span ratio (M/VL_w). Another parameter that contributes to the response variability, in fact, the one that contributes the most, is the record-to-record variability of the input ground-motion. Spectral acceleration at the first-mode period of vibration $S_a(T_1)$ is considered an effective Intensity Measure (IM)[1], nevertheless, among records with the same value of $S_a(T_1)$, there is still significant variability in the level of structural response in a multi-degree-of-freedom sytem[2], especially when subjected to high intensity demand levels that induce large inelastic displacements[25].

To determine the response sensitivity to variations in parameters of macroscopic models, a series of static and dynamic analyses were run in OpenSees [3] through the rescently developed Simcenter [28] platform. The specimen considered herein is RW2 from the Thomsen & Wallace [5]test set. Two finite element models, previously calibrated to simulate the laboratory response, are implemented to assess the variance in response associated to the modeling approach: (i) a fiber forced-based (FIBER) model, and (ii) a Nonlinear Truss (NLT) model. The results presented herein consider material parameter variations such as the reinforcement yield strength (f_y), and the concrete strength (f'_c). The impact of the variations of the equivalent damping ratio (ζ), the mass, and the ALR in the response is also studied. To isolate the impact of the record-to-record variability, a ground motion set whose variance is reduced close to zero is employed. These records were previously selected by Arteta et al (2018) [6] to tightly match (TM) a target uniform hazard spectrum (UHS).

This paper presents a methodology to statistically quantify the impact of the variation of the modeling parameters in the structural response of an isolated cantilever RC wall. This is a first approach to focus the modeling efforts on calibrating only those parameters that most impact the structural response for future research.

2. Reliability of Structural Walls

The aim is to model the structural response variance associated to the uncertainty in material properties, damping characteristics, axial load, and mass. Samples of the parameters are generated by Monte Carlo methods for simulating thousands of realizations of the model [7]. Sensitivity analyses provide a straightforward method for interpreting the effects of modeling uncertainties on response quantities of interest (Liel et al (2009) [8], Porter et al (2002) [9], Lee and Mosalam (2005)[10], Ibarra and Krawinkler (2005) [11], Aslani (2005) [12], and Esteva and Ruiz (1989) [13]). The effect of each random variable (RV) on the structural response is first evaluated by varying each modeling parameter, one-at-a-time, and recording the corresponding structural response. The realizations of each RV follow a probability density function (PDF) which describes the frequency of its occurrence according to data found in the literature which describes the empirical behavior. Later, all RV are varied at the same time, in a simulation of several thousands of realizations, to obtain a sense of the total plausible variance in the structural response.

2.1 Sources of Uncertainty

Ground motion

Selection of earthquake ground motion (GM) records is a topic of ongoing research given the large uncertainty inherent to the ground acceleration production process. For example, for a given scenario of magnitude, distance and soil conditions, the total standard deviation (σ_{ln}) of the GMs predicted by the NGA-West2 GMPEs is around 0.7 in logarithmic units. This means that the GMs between +/- 1σ_{ln} of the median

may differ by a factor of 4. For the seismic response of RC component and systems, Lee and Mosalam (2006)[14] reported that the ground motion variability is a more dominant source of uncertainty affecting global engineering demand parameters (EDP), as compared to the variability in response induced by the variance in structural properties.

To isolate the impact of the record-to-record variability in structural response, a set of twenty accelerograms whose 5%-damped response spectrum tightly match a target UHS are employed (see Figure 1a). These records are denoted the TM set and were previously selected and modified by Arteta et al (2018) [6] to test the impact of ground motion selection methods in the structural response of special moment frames in California. They have the main characteristic of exhibiting a variance close to zero (see Figure 1b). To test the impact of the GM intensity in the structural response, the GM set was increasingly scaled so that the median of the spectral acceleration was $Sa(T_1)$ = 0.05 g, 0.10g and 0.20 g. The first intensity level only imposed elastic demand on the wall, while the third level of demand pushed it considerably within its inelastic range of response. With each record, a nonlinear response history analysis (NL-RHA) is conducted to estimate the EDP of interest.

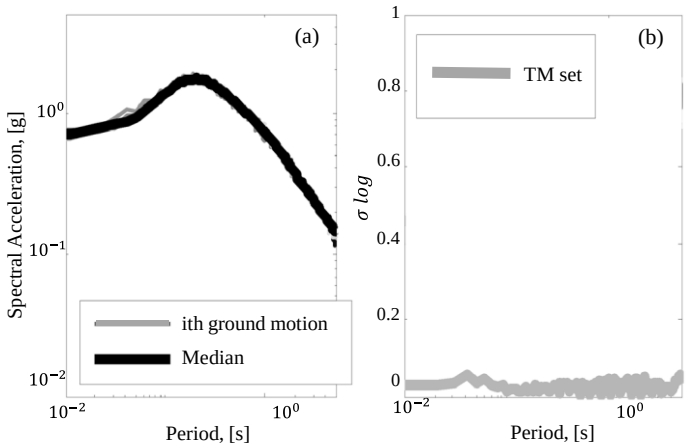

Figure 1. Selected ground motions: (a) 5%-damped spectral accelerations; (b) variability (in log units) of selected ground motions (after Arteta et. al (2018) [6]).

Reinforcing steel yield strength

The reinforcing steel yield strength (f_y) is considered here as a source of uncertainty for academic purposes, although it variance is small thanks to the high-quality standards of the steel production process. According to Mirza and MacGregor (1979) [15], there are several sources that cause the variation in yield strength, such as: (1) variation in the strength of the material itself; (2) variation in the cross section area of the bar; (3) effects of the loading rate; and (4) definition of the strain at yield strength. Previous studies reporting on the variability in f_y, were carried out by Mirza and MacGregor (1979) [15], Bournonville et al (2004) [16], Nowak & Szerszen (2003) [17], Allen (1972) [18]. In summary, these studies show experimentally that the PDFs that best fit the variation of this parameter are Normal and Beta with a coefficient of variation (COV) for grade 60 steels between 3.5% and 6%.

In this study, the Normal PDF used by Mirza and MacGregor (1979) [15] , with a coefficient of variation (COV) of 4%, is selected. Equation 1 describes the functional form of such PDF:

$$PDF = \frac{1}{\sigma_x\sqrt{2\pi}} exp\left[-\frac{1}{2}\left(\frac{x-\mu_x}{\sigma_x}\right)^2\right] \quad (1)$$

where μ_x is the mean and σ_x is the standard deviation.

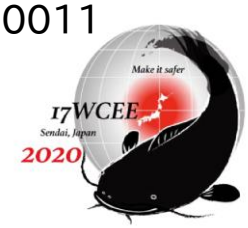

Unconfined concrete compressive strength

The main source of variation in the compressive strength of concrete (f'_c) are the variations in the material properties (e.g. strength and geometry of the rock, cement setting characteristics), in the proportions of concrete mix, and variations in the mixing process, transportation and placing. Mirza and MacGregor (1979) [19] and Nowak et al. (2008) [20] fit the f'_c relative variations with a Gaussian PDF. Studies in the United States report a range of 0.1 to 0.2 for the COV of compressive strength of concrete [21]. Selected COV for this study is 0.15.

Damping

The equivalent damping ratio (ζ) has been usually selected to be 5%, but may vary for the same structure between ground motions of different or equal intensity, depending on the hysteretic energy dissipated by the components. According to a study conducted by Porter [9], the variability for this parameter can be fit through a Normal PDF with a COV in the range of 0.3 to 0.4. In this study the lower bound is select, e.g. COV of ζ is 0.3.

Mass

The mass (M) of the wall is a source of uncertainty because the dimensions of the structural components are not exactly the same as provided in the design documents, and the unit weight of the materials is not perfectly known, which can significantly affect the dead load [9]. A Normal PDF proposed by Ellingwood et al. (1980) [22] is implemented herein with a COV of 0.10.

Axial Load

The variability in the axial load of a wall has some sources of uncertainty such as the geometric variations of the structural elements, impediment to obtaining exact unit weights of the construction materials, and finally the additional load it acquires during its service life when it acts as a resistance system within a building. Ellingwood et al. (1980) [22] describe the variation of the axial load using a Normal PDF and recommends a COV of 0.10.

Table 1 summarizes the mean and COV of the parameters varied in this article. The mean values of f_y, f'_c and AL correspond to those reported by Thomsen & Wallace [5] and used by Arteta et al [24] for simulating experimental results. Mean value for ζ follows standard inelastic modeling practice [23]. The mean value for M is selected to produce a 1 s first-mode period for dynamic analysis purpose.

Table 1 - PDF used to create variability in model inputs

Parameter	Distribution	Mean	COV
fy (MPa)	Normal	434	0.04
f'c (MPa)	Normal	44	0.15
Damping, ζ	Normal	0.025	0.30
Mass, *M (KN*s²/in)*	Normal	16	0.10
Axial Load, *AL (KN)*	Normal	378	0.10

3. Specimen Calibration and Benchmark Response

Before varying the modeling parameters, the empirical results of the RW2 specimen were simulated with the FIBER and the NLT models. These two models produce benchmark results for latter comparison. Their geometry, reinforcement detailing, and modeling parameters are described next.

3.1 Geometry description and model formulation

Specimen RW2 has 1200 mm in length (l_w), 3650 mm in height (h_w), and 100 mm in thickness (t_w) (see Figure 2a). The axial load ratio ($P/A_g f'_c$) is 7%, where P = AL, and A_g is the gross cross section area of the specimen. The shear span ratio (M/Vl_w) is 3.13, hence the specimen is considered as slender. The longitudinal

reinforcement ratio of the boundary elements ($\rho_{v,BE}$) is 2.93%, and the transverse and vertical steel ratio of the wall web are $\rho_{h,web} = \rho_{v,web} = 0.33\%$.

3.2 Analytical model calibration under reversed cyclic loading protocol.

Figure 2a and b show the discretization of the mathematical models implement to test the variability in the structural response associated to modeling techniques. A main difference between both modeling approaches is that the force-based FIBER formulation is based on the classical beam Euler-Bernoulli theory in which plane sections remain plane before and after the deformation, and shear distortions are not accounted for. On the other hand, the NLT model can simulate inelastic shear-flexure interaction, and the compression field is accounted for by the diagonal elements. In the uncracked state, the stiffness of the NLT model is larger than that of the FIBER model due to the overlapping of concrete areas promoted by the discretization.

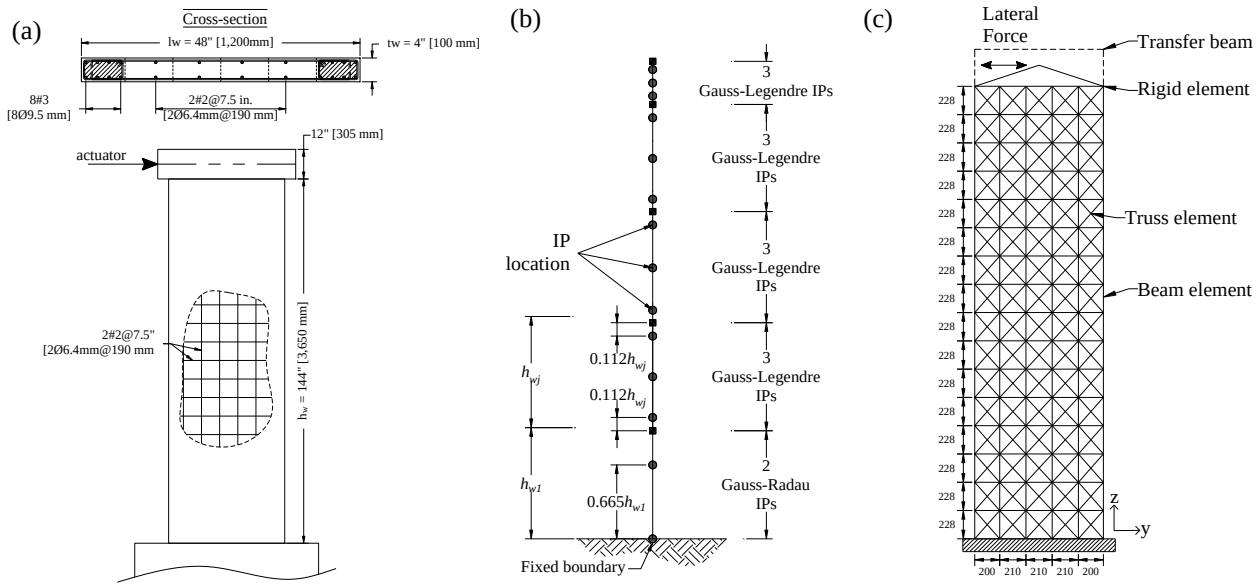

Figure 2. (a) Geometry and reinforcement detailing of RW2; (b) OpenSees FIBER model and (c) NLT model.

The calibration of the parameters of the FIBER and the NLT models are consistent with those in Arteta et. al (2019) [24]. Figure 3 compares the experimental results of the reversed-cyclic loading protocol with the simulations performed in OpenSees for each model. There is an overall agreement between the experimental and simulated response in terms of strength, displacement, and energy dissipation for both models.

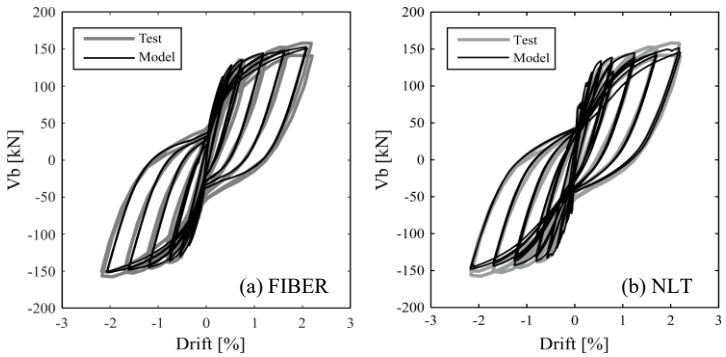

Figure 3. Load-displacement responses simulated by the FIBER model (a) and the NLT model (b) (after Arteta et. al (2019) [24]).

3.3 Benchmark dynamic responses

The sensitivity analysis of the structural response is performed in the dynamic domain with the models used to create the results in Figure 3. The mean mass and damping ratio in Table 1 are assigned to the models for generating the benchmark response under the TM set with the three scaling factors described before. Figure 4 shows the relative frequency of maximum RDR for each model and demand level, along with the median value and the COV. These results will be referred to as the benchmark results in the reminder of the document. The median response of the NLT model is between 8 and 11% smaller than that of the FIBER model, with the difference being larger for the lower demand levels. This is consistent with the NLT model having a larger uncracked stiffness, and the models being excited within their elastic range of response. It is worth noting that albeit having almost no variance, the TM ground motion set produces structural response with COV in the range 0.11 to 0.24, being larger for ground motion intensity levels that yield the model. This is so because $S_a(T_1)$ loses its performance as predictor of the structural response as the intensity increases and the structure respond inelastically [25] [26].

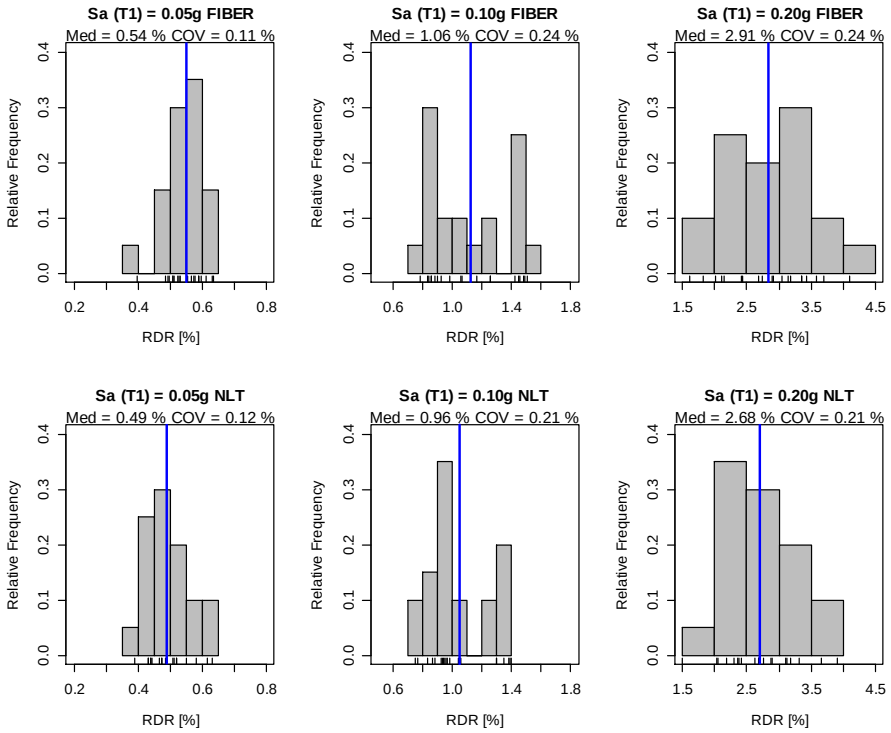

Figure 4. RDR response histograms for each scale factor level and each OpenSees analytical model.

4. Methodology

The application EEUQ [27] developed by the SimCenter is selected in the study for its capability of running thousands of NL-RHA in parallel through the DesignSafe platform[4]. Two approaches were followed to estimate the impact of the variability of modeling parameter in the structural response (i.e., the RDR of the wall): (i) the OAT (one-at-a-time) method, varies each of the 5 parameter in Table 1, one-at-a-time, sampling its distribution, and then running a simulation for a GM of the TM set. Each modeling parameter is sampled 500 times for each model type, each GM, and each scaling factor; (ii) the ATST (all-at-the-same-time) method comprises 10,000 NL-RHA runs per model and scaling factor, in which all five modeling parameters are sampled at once in each realization. A total of 360,000 NL-RHA were performed for this study. The 6 models created are organized as follow indicating the scaling factor and the model type: "Sa(T_1)=0.05 FIBER"; " Sa(T_1)=0.05 NLT"; " Sa(T_1)=0.10 FIBER"; " Sa(T_1)=0.10 NLT"; "0. Sa(T_1)=0.20 FIBER"; "

Sa(T_1)=0.20 NLTM". For each of these models samples were generated considering all of the GM time series, using the Latin Hypercube Sampling (LHS) methodology. Figure 5 shows result of the maximum RDR for the FIBER model obtained for 2 GMs of the OAT subset and the Sa(T_1) = 0.20 g scaling factor. In the figure, each row corresponds to a single GM, and the columns are the RDR response when each parameter is varied. It is worth noting that the median is stable among variation of parameters in a single GM, indicating no bias is introduced by the sampling approach.

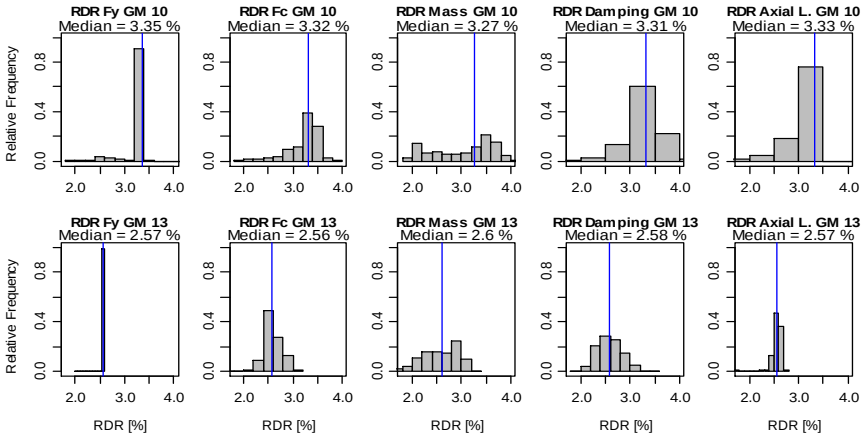

Figure 5. Histogram of the response obtained GM from the OAT subset and Sa(T_1) = 0.20 FIBER sub-model.

For determining the sensitivity of the structural response to variations of each modeling parameter, the "*Relative Deviation Ratio*" (θ) [29], is estimated. Equation (2) describes this index, which relates the COV of the model response (e.g. COV of the RDR) to the COV of the parameter.

$$\theta = \frac{COV_{model}}{COV_{parameter}} \tag{2}$$

The interpretation of *Relative Deviation Ratio* is as follows: consider two parameter distributions, one wide and the other narrow that produce the same COV_{model}, intuitively one can say that the model is more sensitive to the input parameters of the narrower distribution. A large value of θ indicates that the model is sensitive to that parameter.

4. Results

4.1 OAT method

Figure 6 shows the results of the 6 models organized as follows: (i) the x-axis represent each one of the 20 GMs of the TM set, organized according to the median response each one induces on the structural models; (ii) the y-axis is the ratio between the median response under each parameter variation and the deterministic response under each GM; this index indicates how the median stochastic response deviates from the benchmark response. (iii) the size of the bubble indicates the COV of the structural response under each parameter variation; (iv) the color of each point indicates the parameter varied. For example: for the Sa(T_1)=0.05 FIBER model, the first tick of the x-axis is GM N°17, the y-axis shows that all parameter variations produced similar stochastic deviations of the median from the benchmark response, but the response COV induced by variations in the mass (M), the axial load (AL), and damping ratio, ζ is larger. This is a common observation for all the models and scaling factors considered. It is worth noting that the steeper average slope of the FIBER subset in Figure 6 indicates that the record-to-record variability impacts

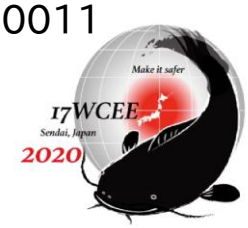

more the FIBER model than the NLT model, which seem more stable as the ground motion intensity increases.

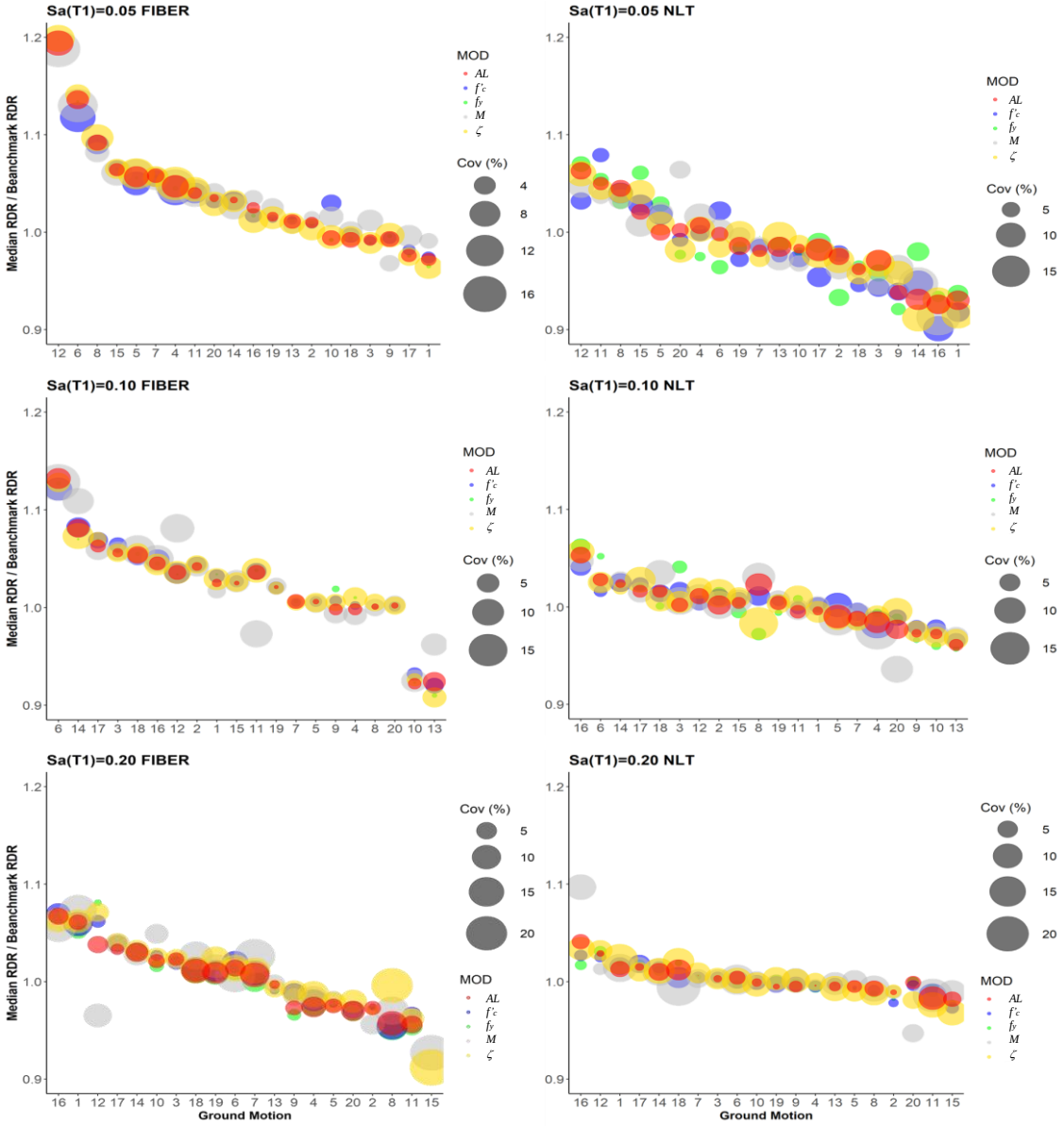

Figure 6. Response obtained from the sub-models by performing one-at-a-time simulations.

The sensitivity index θ was estimated for each model and a tridimensional surface summarize the results in Figure 7. For the case-study example, results indicate that parameters f_y and M generate the largest impact on the RDR response. It is worth recalling that the COV_{fy} = 4% and COV_M = 10%, meaning that small variations in f_y and M are generating great impact in the RDR response, as compared to those of, for example, the ζ variations, which produce large dispersion in the structural response (see Figure 6), but also have a wider PDF. Also note that θ increases with ground motion intensity, as the RDR variance increase in the inelastic range of response [25]. Except for the f_y variations at the largest scaling factor (i.e. $S_a(T_1)$ = 0.2 g), θ values for the NTL model are larger than those of the FIBER model, indicating a larger response variance as confirmed in Figure 6.

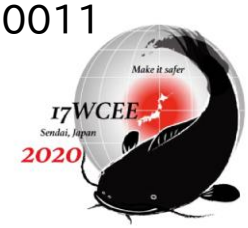

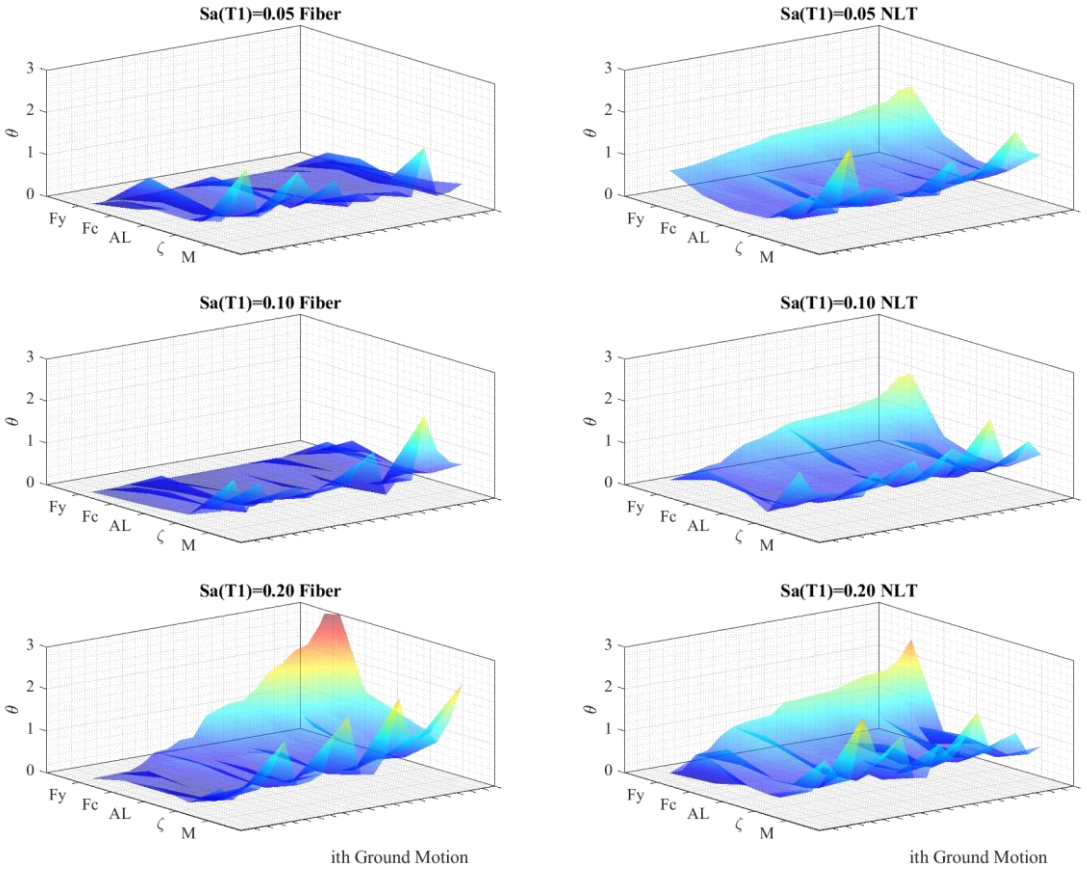

Figure 7. Surfaces generated with the θ sensitivity index values for each of the sub-models.

4.2 ATST method

The full structural response variation given the dispersion of the modeling parameters is obtained by performing 10,000 NL-RHA per scaling factor and model type, sampling all modeling parameters at once, including the input ground motion. Figure 8 shows the structural response data organized in Violin Plots describing the dispersion for each of the models considered. The benchmark response for each GM is also presented for context. The data is organized in descending order according to their median values to show how the record-to-record variability impacts the response. Horizontal dotted lines indicate the range over which the median varies.

Results in Figure 8 confirm that the dispersion in the response increases with GM intensity. Furthermore, the record-to-record variability shown indicates that elastic spectral coordinates might not be the best predictor of the structural response under study. For instance, although all GMs of the TM set have identical spectral coordinates, the ratio between de maximum median response and the minimum median response is between 1.6 and 2.4, being larger for increasing scaling factors. The results also confirm that the NLT model exhibits smaller median RDR values than those of the FIBER model, although the difference reduces as the intensity level increase because the inherent larger initial stiffness has less impact in the response.

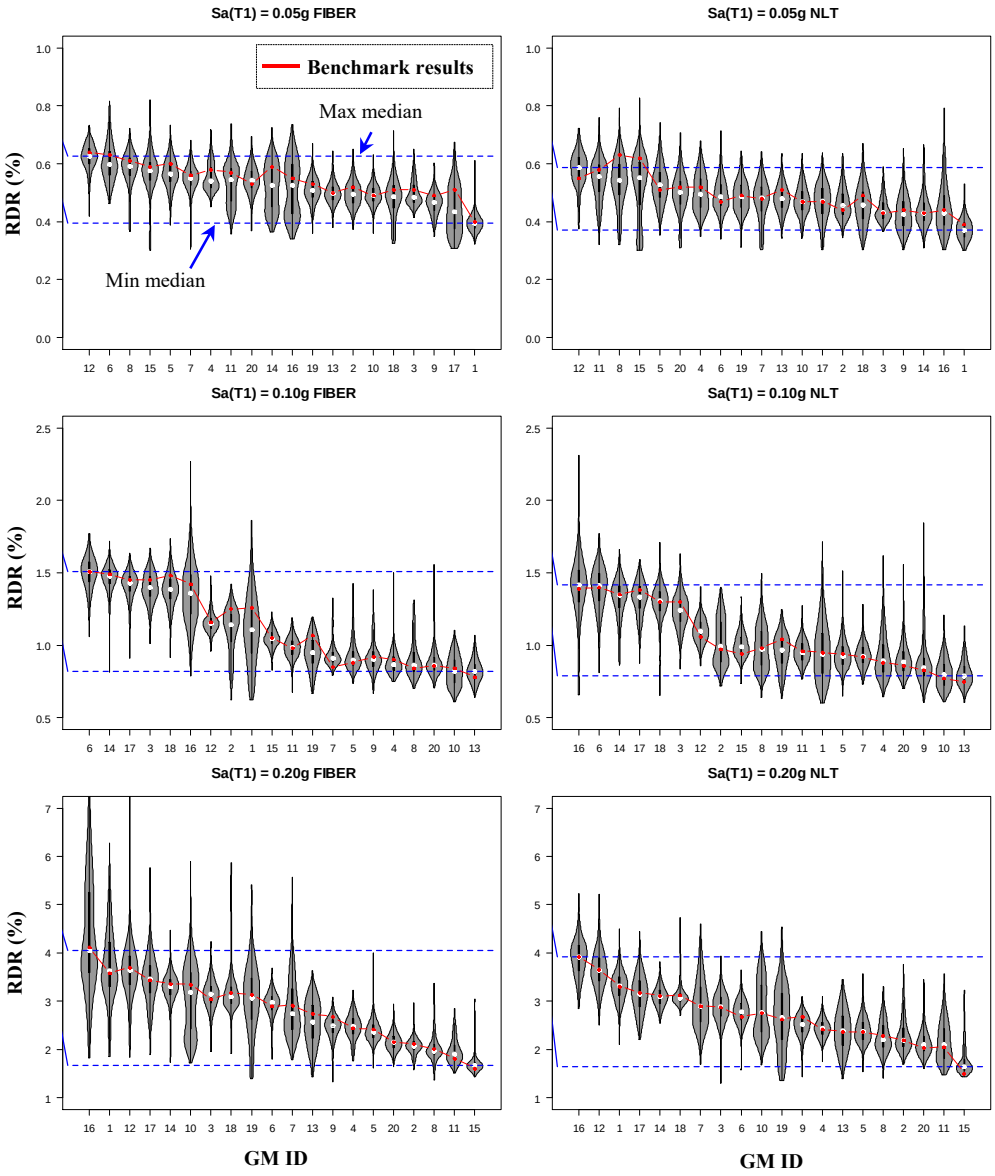

Figure 8. Violin plots of the RDRs obtained for each of the models, varying all the parameters at the same time.

Figure 9 shows the results of the ATST method for the three scaling factors aggregating the results of the FIBER and the NLT model. Also presented are the median, and minimum and maximum response of the benchmark results also aggregating both models. It is noted that the minimum and maximum deterministic benchmark results capture between 86% and 95% of the stochastic results, indicating that the record-to-record variability is the largest source of variability when modeling RC walls as the one considered here. This is so, because there is no GM variation between the benchmark and the stochastic results. It is also noted that RDR values on the right tail of the distributions are mainly contributed by the FIBER model.

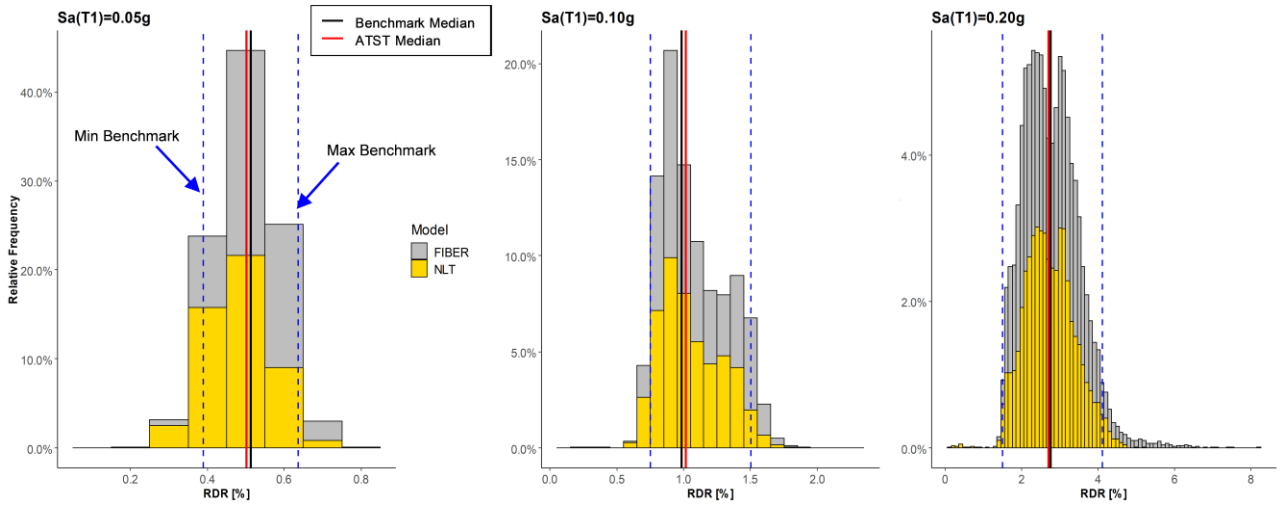

Figure 9. RDR response histogram for the ATST method, considering the FIBER and NLT model

5. Conclusion

The article presented a simple methodology to estimate the influence of modeling parameters in the behavior of an isolated slender shear wall as subject of analysis. The influence is calculated using the "Relative Deviation Ratio" which is the ratio between the variance of the parameters and the structural response variance. For the case study and modeling parameters presented, variance in the yield strength and mass of the model generated the greatest impact in the structural response. This means that the model is more sensitive to changes in f_y and mass. Nevertheless, the bubble charts showed that the highest COV in the RDR response was induced by the damping ratio given its large dispersion. A ground motion set with no variability in their spectral coordinates was selected to isolate the record-to-record variability effects. Nevertheless, as the problem is highly nonlinear, the results showed that the ground motion selection has a great impact in the structural response observed. Future research must expand the number of modeling parameter studied to have a broader sense of their importance when calibrating mathematical models representative of actual structures.

6. Acknowledgements

The authors would like to thank Gustavo Araujo Rodriguez and Andres Torregroza Castro for their support in the analytical calibration of the OpenSees approach models used for the RW2 specimen.

7. Copyrights

8. References

[1] Shome, N., Cornell, C. A., Bazzurro, P., & Carballo, J. E. (1998). Earthquakes, Records, and Nonlinear Responses. 14(3), 469-500. doi:10.1193/1.1586011.

[2] Baker, J. W., & Allin Cornell, C. (2005). A vector-valued ground motion intensity measure consisting of spectral acceleration and epsilon. 34(10), 1193-1217. doi:10.1002/eqe.474.

[3] McKenna, F., Fenves, G. L., Scott, M. H., & Jeremic, B. (2000). Open system for earthquake engineering simulation (OpenSees) (version 3.1.0). *Pacific Earthquake Engineering Research Center, University of California, Berkeley*.

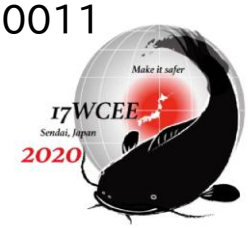

[4] Rathje, E. M., Dawson, C., Padgett, J. E., Pinelli, J.-P., Stanzione, D., Adair, A., . . . Mosqueda, G. (2017). DesignSafe: New Cyberinfrastructure for Natural Hazards Engineering. 18(3), 06017001. doi:doi:10.1061/(ASCE)NH.1527-6996.0000246
[5] Thomsen, J. H., & Wallace, J. W. (2004). Displacement-Based Design of Slender Reinforced Concrete Structural Walls; Experimental Verification. 130(4), 618-630. doi:10.1061/(ASCE)0733-9445(2004)130:4(618)
[6] Arteta, C. A., Mazzoni, S., & Abrahamson, N. A. (2018). Evaluating ground-motion modification procedures with the Conditional Scenario Spectra. In Proceedings, 11th National Conference on Earthquake Engineering (pp. 25-29).
[7] Warner, R. F., & Kabaila, A. P. (1968). Monte Carlo study of structural safety. Journal of the Structural Division, 94(12), 2847-2860.
[8] Liel, A. B., Haselton, C. B., Deierlein, G. G., & Baker, J. W. (2009). Incorporating modeling uncertainties in the assessment of seismic collapse risk of buildings. *Structural Safety, 31*(2), 197-211.
[9] Porter, K. A., Beck, J. L., & Shaikhutdinov, R. V. (2002). Sensitivity of Building Loss Estimates to Major Uncertain Variables. *18*(4), 719-743. doi:10.1193/1.1516201
[10] Lee, T. H., Mosalam, K. M. J. E. e., & dynamics, s. (2005). Seismic demand sensitivity of reinforced concrete shear-wall building using FOSM method. *34*(14), 1719-1736.
[11] Ibarra, L. F., & Krawinkler, H. (2005). *Global collapse of frame structures under seismic excitations*: Blume Center TR 152, Stanford University.
[12] Aslani, H., & Miranda, E. (2005). Probabilistic earthquake estimation and loss disaggregation in buildings. In: Stanford, CA, Stanford university, The John A. Blume Earthquake Engineering.
[13] Esteva, L., & Ruiz, S. E. J. J. o. S. E. (1989). Seismic failure rates of multistory frames. *115*(2), 268-284.
[14] Lee, T.-H., & Mosalam, K. M. (2006). *Probabilistic seismic evaluation of reinforced concrete structural components and systems*: Pacific Earthquake Engineering Research Center.
[15] Mirza, S. A., & MacGregor, J. G. J. J. o. t. S. D. (1979). Variability of mechanical properties of reinforcing bars. *105*(ASCE 14590 Proceeding).
[16] Bournonville, M., Dahnke, J., & Darwin, D. (2004). *Statistical analysis of the mechanical properties and weight of reinforcing bars*.
[17] Nowak, A. S., & Szerszen, M. M. J. A. S. J. (2003). Calibration of design code for buildings (ACI 318): Part 1-Statistical models for resistance. *100*(3), 377-382.
[18] Allen, D. E. (1972). Statistical study of the mechanical properties of reinforcing bars. *Building Research Note, 85*, 22.
[19] Mirza, S. A., MacGregor, J. G., & Hatzinikolas, M. J. J. o. t. S. D. (1979). Statistical descriptions of strength of concrete. *105*(6), 1021-1037.
[20] Nowak, A. S., Szerszen, M. M., Szeliga, E., Szwed, A., & Podhorecki, P. J. S., Portland Cement Association, Stokie, IL. (2008). Reliability-based calibration for structural concrete, phase 3.
[21] Francisco J., P. (2019). *Efficient Computation of Accurate Seismic Fragility Functions Through Strategic Statistical Selection*.
[22] Ellingwood, B., Galambos, T. V., MacGregor, J. G., & Cornell, C. A. (1980). *Development of a probability based load criterion for American National Standard A58: Building code requirements for minimum design loads in buildings and other structures* (Vol. 13): US Department of Commerce, National Bureau of Standards.
[23] ATC. (2017). Guidelines for Nonlinear Structural Analysis for Design of Buildings Part I: National Institute of Standasrds and Technology.
[24] Arteta, C. A., Araújo, G. A., Torregroza, A. M., Martínez, A. F., & Lu, Y. J. B. o. E. E. (2019). Hybrid approach for simulating shear–flexure interaction in RC walls with nonlinear truss and fiber models. doi:10.1007/s10518-019-00681-6
[25] Arteta, C. A., and Abrahamson, N. A. (2019). Conditional Scenario Spectra (CSS) for Hazard-Consistent Analysis of Engineering Systems. *Earthquake Spectra, 35*(2), 737-757. doi:10.1193/102116eqs176m
[26] Baker, J. W., and Cornell, C. A. (2006). Spectral shape, epsilon and record selection. *Earthquake Engineering & Structural Dynamics, 35*(9), 1077-1095. doi:10.1002/eqe.571
[27] Frank McKenna, Wael Elhaddad, AdM Zsarnoczay, Michael Gardner, & Charles Wang. (2019, June 29). NHERI-SimCenter/EE-UQ:Release v1.2.0 (Version v1.2.0). Zenodo. http://doi.org/10.5281/zenodo.3262287
[28] "SimCenter Computational Modelingand Simulation Center." *DesignSafe*, 12 Feb. 2020, simcenter.designsafe-ci.org/.
[29] Hamby, D. M. (1995). A comparison of sensitivity analysis techniques. *Health physics, 68*(2), 195-204.

